

RESEARCH PAPER



Decision support system for managing flooding risk induced by levee breaches

Lorenzo Scopetani^a, Simona Francalanci^a, Enio Paris^a, Leonardo Faggioli^b and Jacopo Guerrini^b

^aDepartment of Civil and Environmental Engineering, University of Florence, Firenze, Italy; ^bConsorzio di Bonifica 3 Medio Valdarno, Firenze, Italy

ABSTRACT

Managing the levee system of a river network is an essential aspect to reduce the flood risk and protect communities and urbanised areas. Too many times, the viewpoint of the managing institution in charge of the restoration of river levees is of an emergency type so that the restoration works are conducted only after flood occurrence, without the consideration for a complete and necessary overview of priority criteria at a basin scale. The present work aims to develop a basin-scale methodology to analyse the current state of the Ombrone Pistoiese River (Italy) levees, so as to identify targeted solutions for breakage prevention. By applying a vulnerability index, producing maps of flooded areas and counting the exposed elements induced by levees breaks, this study wants to provide a decision support procedure able to define a priority scale of interventions.

ARTICLE HISTORY

Received 30 July 2021
Accepted 31 July 2022

KEYWORDS

Levee breach; flood mapping; basin-scale management; seepage; slope stability

1. Introduction

The protection of urbanized areas from hydraulic risks is one of the main goals of river basin management. The frequency of high-intensity rain events is growing, causing extensive damage to people and infrastructures in the flooded area, seriously compromising economic development and endangering the economic activities of the Community (CE, 60/2007, n.d.; Huston, 2011).

In this context, there are two common types of interventions for flood risk reduction (Mazzoleni et al., 2017; McBain, 2012): structural interventions, such as the construction of hydraulic structures or reinforcement of the existing ones (dams, levees) (Michelazzo et al., 2018), and non-structural interventions, which include plans or laws that discourage building near the river, or actions for prevention, protection, and preparedness (Minea & Zaharia, 2011). Structural interventions can be classified into active interventions, which modify the flood hydrograph, such as flood storage areas or artificial reservoirs, and passive interventions, such as embankment systems, which reduce the occurrence of flooding by increasing the carrying capacity of the river channel (Ligato, 2003; Sattar et al., 2019).

Under the EU Floods Directive (CE, 60/2007, n.d.), the creation of risk and hazard maps is essential in river risk management. Levees play a major role in reducing flooding areas, but it is important to note that they are usually considered as non-collapsing structures, underestimating the potential flooding in case of levee failure or breach (Barbetta et al., 2017; Mazzoleni et al., 2014; Solari et al., 2014). Moreover, some embankment systems were built many centuries ago (Tourment et al., 2018), and because of significant changes in land development and environmental conditions, they may no longer be able to withstand the load. For this reason, it is crucial to analyse the stability of these earthen structures and consider their possible collapse with the consequences they may generate (Colman et al., 2016).

In recent years there have been many harmful events worldwide as a result of levee breaks (Van et al., 2019). For example, the London canal breach in Louisiana in 2005 (Collins et al., 2009), the Serchio River (2009) and Secchia River (2014) in Italy, the Mississippi River breaches of the Pin Oak levee in Winfield 2019, and, more recently, the massive flooding in Germany (2021), causing extensive economic damage and inconvenience to the population. For this reason, the prediction of risk due to hydraulic structure failure is essential (Dazzi et al., 2019; Vacondio et al., 2016; Viero et al., 2013).

Within the scope of river management, an appropriate methodology for supporting decision tools must include the risk induced by potential levee failure. To analyse the stability of the embankments, first, it is necessary to have adequate knowledge of the territory, of the structural changes that the embankments have undergone over time and the historical harmful events for the investigation and prediction of possible recurring critical issues based on a historical-inventory type approach (Ko & Kang, 2018; Northern Apennine District Basin Authority, 2016). The second fundamental step is to investigate the main collapse mechanisms such as seepage processes through the embankment and mass instability of banks (Da Deppo et al., 2011). The prediction of an embankment collapse and the evaluation of the induced consequences are very complex issues. In the literature, several criteria for analysing the interaction between water levels and the saturation trend in the embankment body (Marchi, 1957) are available, giving indications of the phenomena affecting the instability process. The main mechanisms of embankment breakage essentially concern phenomena such as overtopping, seepage, erosion and mass instability (Colleselli, 1994; Serre et al., 2008). The search for the criticalities that cause embankment breaches can be challenging since phenomena such as seepage or the presence of animal dens occurring underground is not

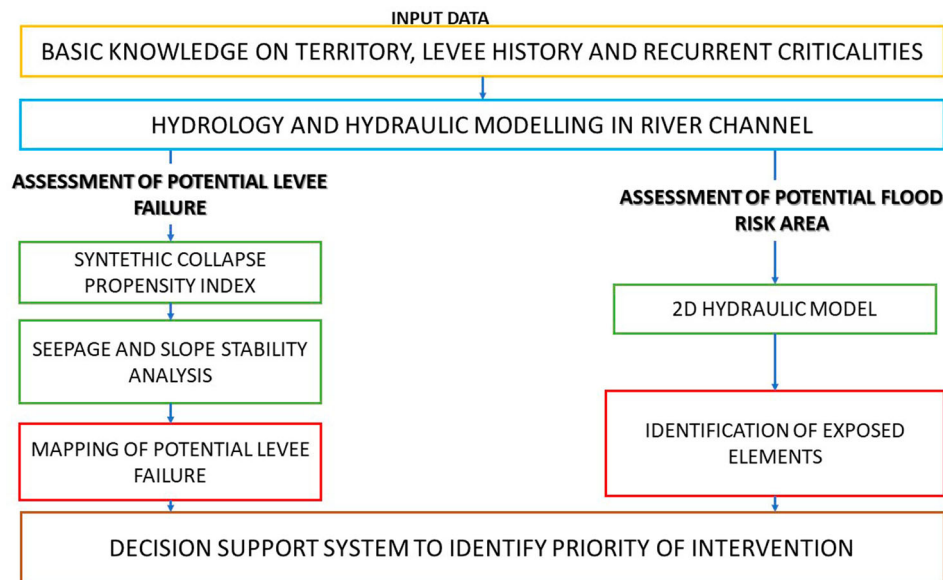


Figure 1. Flowchart of the proposed methodology.

visible on the embankment body but are among the leading causes of embankment breaches (Camici et al., 2014; Orlan-dini et al., 2015; Sofia et al., 2017; Viero et al., 2013). The analysis of breaches caused by overtopping phenomena is highly studied, and many methods of analysis have been proposed, such as fragility curves (D’Oria et al., 2019; Hall et al., 2003;), which however do not consider the seepage phenomenon (Mazzoleni et al., 2014, 2017). Some studies have developed fragility curves considering seepage as one of the main causes of embankment breaches (Barbetta et al., 2017; Vorogushyn et al., 2009;). Their application is essential for this type of analysis (Barbetta et al., 2017; Camici et al., 2014;), but only seepage analyses are considered, and not their consequences. Studies on this topic very often involve local-scale analyses or reproductions of the damaging event, and not basin-scale predictive analyses (Michelazzo, 2013). At present, there are studies on specific cases of embankment breakages (Mazzoleni et al., 2014), aimed at reproducing individual events at the local scale, based on models of variable complexity (Vorogushyn, 2010). These studies are based on one-dimensional models (Zhang et al., 2013), 1D/2D coupled models (Todini, 2000) or 2D models (Ferrari et al., 2020; Mazzoleni et al., 2014;), depending on what has been investigated. On the other hand, to the Author’s knowledge, no methodology for assessing hydraulic risk from embankment collapse is available at the basin scale (Solari et al., 2014).

In this context, the present study aims to develop and implement a methodology to support the decision system in a highly urbanized river basin subjected to flood risk induced by levee breach. To this aim, the methodology is applied to the case study of the Ombrone Pistoiese River, but it can be easily extended to any other river catchment, following the procedure described in section 2. The levee breach potential occurrence is evaluated based on three indexes (Solari et al., 2014). The first one considers the possible internal erosion caused by seepage processes using the Marchi equation (1961), while the other two are based on the cross-section geometry. The proposed methodology has been applied to the river basin of the Ombrone Pistoiese in Tuscany (Italy).

2. Methodology for a decision support system

This methodology can be applied for the management of extensively embanked rivers, where it is important to correctly plan and allocate economic resources. The purpose of this study is to identify the priorities to allocate the available economic resources considering the intersection of the various steps of the proposed procedure. The methodology considers the subdivision of the total length river into sub-reaches, by assigning them a representative cross-section, where their density is the function of their degree of uniformity of the considered river reach; in theory, if the entire river is completely uniform 100% only one cross-section is needed.

The proposed procedure involves the following steps (see Figure 1):

- *Gathering of all input information* concerning the topographic data, the land use map, the levee system history and all the recurrent historical criticalities.
- *Hydrology and hydraulic models* able to reproduce the flood events for different return period. In particular, the simulation of the flood propagation on the river basin will allow the identification of the main critical events occurring at lower critical return period. This issue is specific for the study area and specific for each river basin.
- *Assessment of potential levee collapse* estimated through three synthetic indexes: the frodo index, the hanging index and the seepage index, calculated at any available river cross-sections. This evaluation is based on the knowledge of geometric and hydraulic data at the basin scale, while at the local scale, if sufficient geotechnical data is available, a detailed levee stability assessment is performed to verify the reliability of the aforementioned synthetic indexes. To this purpose, VS2DTI software for seepage processes (Hsieh et al., 2000), and SSAP software (Borselli, 2018) for slope stability analysis can be used.
- *Assessment of flood risk areas induced by levee breach*, using a 2D hydraulic model (HEC-RAS 5.0.7 software

Table 1. Risk matrix, with the collapse propensity hazard classes on the rows and the exposures classes on the columns.

Risk classes		Exposures classes		
		E1	E2	E3
Propensity to collapse classes	H1	R1	R2	R3
	H2	R2	R3	R4
	H3	R3	R4	R4

in this case), to predict the extent of the flooded areas generated by the levee breach, which is assumed to occur at any cross-section of the river system. Indeed, due to the randomness of levee breach formation, any available river cross-section can be a potential site for such an occurrence. For each site of potential levee breach, the experimental results by Michelazzo (2013) have been used to estimate the outflow hydrographs through the levee breach. Risk has been evaluated by superimposing the flooded area to the map of the exposed elements like inhabitants, buildings, and infrastructures.

– *Decision support system implementation.* In order to provide a preliminary quantification of the risk, a matrix based on the intersection between the value of the exposed elements in the flooded area and the propensity index can be done as shown in Table 1. Assuming the exposed elements would be totally damaged i.e. they completely lose their value, the following exposure and propensity index classes can be identified for the case study of the Ombrone Pistoiese River:

- E1: 0–400 inhabitants, 0–10 km of roads, 0 school;
- E2: 400–1000 inhabitants, 10–20 km of roads, 1–2 school;
- E3: more of 1000 inhabitants, more of 20 km of roads, more of 2 school.
- H1: ‘low’, propensity index between 0.5 and 1.5;
- H2: ‘medium’, propensity index between 1.5 and 3;
- H3: ‘high’, propensity index between 3 and 5;

The above classification can be adapted to other cases on the basis of an assessment based on expertise and specialized knowledge of the specific area.

Hence, the proposed method is able to identify the potential critical cross-section, which has been assumed

here to have risk values in the class R3 or R4. Once these sections have been identified, the decision can be made whether to carry out more detailed analysis and/or to collect additional structural, geotechnical and geometric data

So, the results from the previous steps are used to identify, for every river bank, the priorities to allocate more efforts in terms of survey, monitoring and design intervention.

In the following sections, a detailed description of the proposed methodology is provided, while Figure 1 shows its main flow chart.

2.1. Synthetic collapse propensity index

The propensity of embankments to collapse is evaluated through a synthetic collapse propensity index, which is obtained as a combination of three different indexes that contribute to defining some of the foremost dangerous conditions of an embankment, induced by the permanence of high stage levels in the riverbed which may be critical for the seepage mechanism (Michelazzo et al., 2016). In the following, the critical condition for seepage is assumed to occur when the phreatic line intersects the bank slope on the land side. With reference to Figure 2, the modelling is applied to simplified embankment geometries of trapezoidal shape made of homogeneous and isotropic earth for which porosity and permeability coefficient are known (Michelazzo et al., 2016).

The procedure defines the following parameters (Figure 2):

- $h(x,t)$ water level referred to the impervious layer at x -axis and time t ;
- $h_1(x,t)$ phreatic line referred to the undisturbed water table at the x -axis and time t ;
- $h_0(t)$ water level in the watercourse referred to the undisturbed water level;
- H_f = thickness of the aquifer layer;
- n = soil porosity;
- k = soil permeability;
- T = duration time of the rectangular hydrograph.

Assuming the validity of Darcy’s law, in the hypothesis of homogeneous and isotropic earth, using the mass

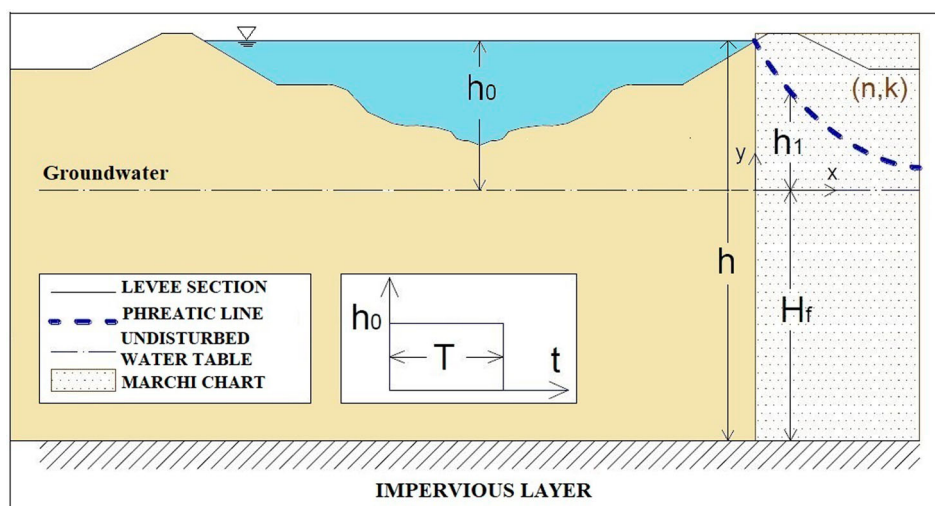


Figure 2. Diagram for the Marchi (1957) model: river cross-section and phreatic line (adapted from Figure 1 in Solari et al., 2014).

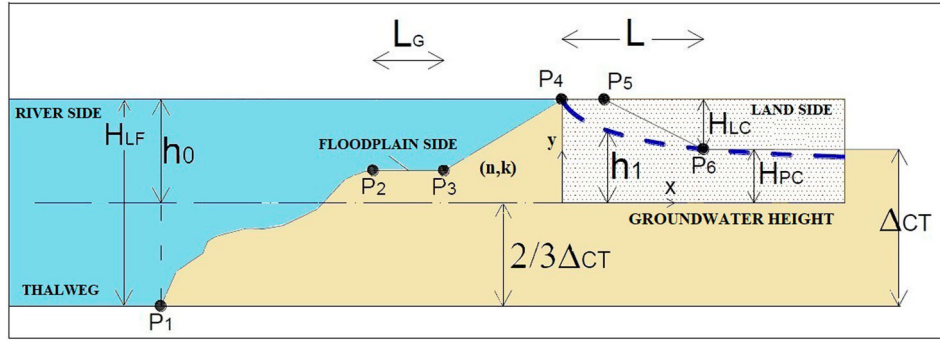


Figure 3. Schematization of the levee with the main parameters (adapted from Figure 2 in Solari et al. (2014)).

conservation and Laplace's laws, and neglecting the phenomenon of capillarity, the maximum phreatic line can be calculated by using the method proposed by Marchi (1957):

$$\frac{h_{\max}(x)}{h_0} = \frac{2}{\pi} \arctg\left(\frac{kT}{nx}\right) \quad (1)$$

Marchi's model is implemented to assess the critical condition for seepage occurring when the phreatic line outcrops on the land side, as shown in Figure 3.

The levee geometry is schematized by the remarkable points (P₃, P₄, P₅, P₆) and by uniform geotechnical characteristics also for the substrate, as one can see in Figure 2. Marchi's model solves the seepage starting from a vertical riverside face, referred to the height of the water levels in the riverbed. This schematization simplifies the model by neglecting the seepage process through the sloping riverside (Solari et al., 2014). Moreover, the height of the aquifer is not known a priori, and it is assumed to be 2/3 of the distance Δ_{CT} between the thalweg and the ground level, following a precautionary choice. When there are cases where the areas outside the levees have lower elevations than the elevations inside the levees (i.e. the thalweg is higher than the elevation of land outside the levees), the aquifer is conventionally assumed to be below the land surface by 50 cm, following empirical evidence. The thickness of the aquifer usually is not known. However, assuming an aquifer thickness of the order of 10–20 m, and considering the base width of the embankments, L in the order of 10–15 m, it is possible to

apply Equation (1) and therefore to use Marchi's model to obtain the major solution of the phreatic line, assuming groundwater thickness as infinite.

The further step in the methodology is the assumption of a water level in the riverbed h_0 up to the top of the embankment (Figure 3) which is kept constant for the entire duration of the rectangular flood hydrograph. Even if this is a simplification of the real flood hydrograph, it aims to consider the most severe load in terms of seepage. By solving the seepage problem in the embankments body for increasing values of duration T , a critical time value, T_{CR} , is obtained for which the phreatic line is able to intersect the land side of the levee. This value is assumed to be the threshold beyond which the hydraulic gradient may cause piping or internal erosion. The critical value T_{CR} , which can also be considered as the levee resistance time, can be estimated by the work of Michelazzo et al. (2016) through the following equation:

$$T_{CR} = \tan\left(\frac{\pi}{2} * \frac{H_{PC}}{H_{PC} + H_{LC}}\right) \frac{nL}{k} \quad (2)$$

2.1.1. Seepage index

The seepage index, I_{SEEP} , is defined as the ratio T_{CR}/T_P where T_{CR} is obtained from Equation (2), and the persistence time, T_P , of the flood event, with a given return period, is known from hydrologic and hydraulic models. The persistence time T_P is here conventionally defined as follows: given the

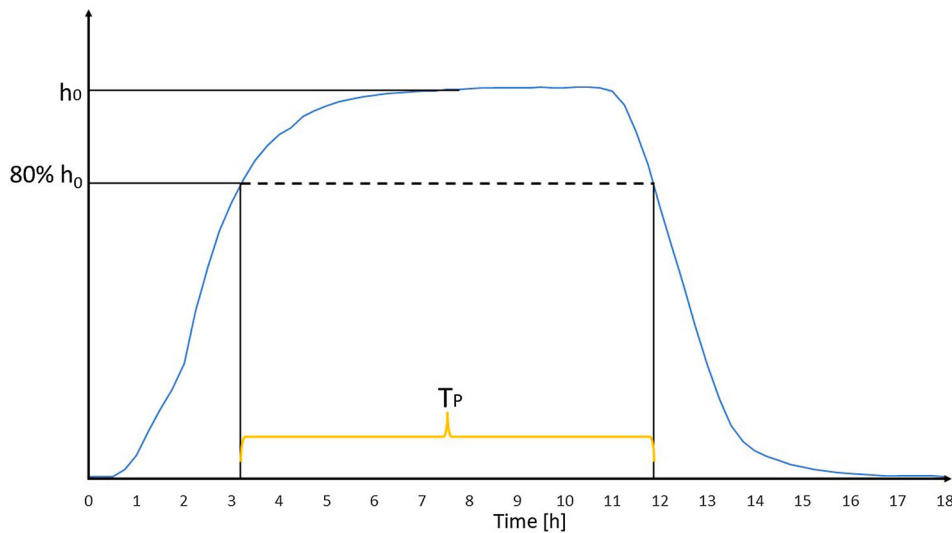


Figure 4. Definition of the persistence time T_P .

stage hydrograph, the persistence time is assumed to be the time for which the water depth is higher than 80 percent of the maximum water depth h_0 contained within the river (see Figure 4). For the given return period, the flood hydrograph to be considered is the one that maximizes T_P . For the sub-reach referred to the cross-section, this condition is assumed to be the most critical in terms of seepage index.

2.1.2. Hanging index

The hanging of a river cross-section occurs when its deepest point (thalweg) has an elevation higher than the landside, thus favouring the phenomena of seepage inside the embankment with possible internal erosion and consequent formation of levee breakage. With reference to Figure 3, the hanging index I_{HA} can be obtained from H_{LF} , i.e. the elevation difference between thalweg and embankment top, and the height of the landside face, H_{LC} . In Table 2, I_{HA} is classed according to the case study of Ombrone River. I_{HA} values are in the range between 0 (a situation in which the height on the land side would be at the top of the embankment, i.e. a river bed totally incised) and 1.

2.1.3. Frolodo index

A levee is termed 'in frolodo' when it is built in transversal continuity with the bank, where, therefore, the floodplain area is absent. In these cases, the levee system is more exposed to the erosion processes other than seepage. To take into account this effect on levee stability, a frolodo index I_{FR} is introduced in terms of the parameters H_{LF} and L_G , respectively riverside face height and width of the floodplain area. The frolodo index will therefore assume greater values when the floodplain extension is more significant than its height. Values of I_{FR} and their classification are shown in Table 2.

2.1.4. Collapse propensity index

The three indexes presented in the previous paragraphs can be combined for a preliminary estimation of the collapse propensity of the embankment induced by seepage phenomena. To this end, a collapse propensity index is here defined as the sum of the three indexes: $i_{TOT} = i_{SEEP} + i_{FR} + i_{PE}$, of which the seepage index has probably more relevance since it has a higher range of variability, and it is directly related to the seepage processes. It is worth noting that the mechanism of overtopping and slope instability have not been taken into account by the propensity index.

For each river cross-section the classification of the collapse propensity index is shown in Table 2.

Table 2. Indexes classification.

Single index classes				
Range (T_{CR}/T)	[0–0.5]	[0.5–1]	[1–5]	[5–10] [10–100]
I_{SEEP}	3	2	1.5	1 0.5
Range (H_{LC}/H_{LF})	$H_{LC} \geq H_{LF}$	$1/2 H_{LF} \leq H_{LC} < H_{LF}$	$H_{LC} < 1/2 H_{LF}$	
I_{HA}	1	0.5	0	
Range (L_G/H_{LF})	$L_G \leq H_{LF}$	$1/2 H_{LF} \leq L_G < H_{LF}$	$L_G > H_{LF}$	
I_{FR}	1	0.5	0	
Global index classes				
$I_{TOT} = I_{SEEP} + I_{HA} + I_{FR}$	$3 \leq I_{TOT} < 5$	$1.5 \leq I_{TOT} < 3$	$0.5 \leq I_{TOT} < 1.5$	
Hazard classes	'High'	'Medium'	'Low'	

2.2. Detailed seepage analysis

The detailed analysis of the seepage process is aimed at carrying out the stability analysis at the local scale as described in the following section. First, it is necessary to choose a reference scenario for a given return time, for which the water levels in the riverbed are entered with their durations, to simulate an unsteady flow model. The water level hydrograph must be coherent with the previous seepage index calculation. The analysis can be conducted using the software VS2DTI version 1.3 developed by the U.S. Geological Survey, which makes it possible to represent the hydraulic characteristics from the van Genuchten, Brooks-Corey, Haverkamp, and Rossi-Nimmo equations, as well as from tabular data (Hsieh et al., 2000). The first step for the construction of the model involves the flow conditions, the setting of the aquifer balance profile for the initial hydraulic conditions, and the definition of the boundary condition using the hydrographs of the water levels. These are set by assuming a two-dimensional problem, a domain divided into layers and lenses, soil belonging to the single homogeneous and isotropic units, the total head on the riverside interface variable over time, total head on the valley contour constant and equal to the height of the water table. Finally, the model needs geomechanical parameters, assumed or taken from penetrometric tests, and the choice of the calculation equation; in this case, the van Genuchten equation is used (van Genuchten, 1980).

2.3. Slope instability

The geotechnical approach to slope stability analysis involves the study of rupture along a surface, or a band including such surface, which occurs when the destabilizing forces (shear forces on the slope) exceed the stabilizing forces (shear resistance of the material), i.e. when the Safety Factor SF is less than 1. In addition to the usual hypotheses of flat, rigid-plastic deformation, drained or undrained shear strength, another simplifying hypothesis is proposed for examining the situation at slope failure, i.e. SF is considered constant along the rupture surface (Colleselli, 1994). Considering the results obtained from other comparative studies on stability analysis methods (Nash, 1987), it can be concluded that methods that satisfy both the equilibrium of forces and moments, Morgenstern and Price (1965) and Janbu (1973) provide accurate results ($\pm 5\%$) for this type of slope analysis.

In this step, it is important to evaluate the safety factor and compare it with the regulatory limits. This was performed using the SSAP software, version 5.0.2, developed by Borselli (2018). The model requires the insertion of the geometry of the levee section, the phreatic line as obtained from the previous section, with the possibility to take into account an overload at the top of the embankment due for instance to the presence of machinery for maintenance activity.

2.4. 2D hydraulic model for flood risk mapping

The methodology includes the evaluation of the flooded areas generated by any levee breach associated with each cross-section, in order to assess the potential damages of the exposed elements (population, buildings, infrastructures). The spatial domain of the 2D model is confined by

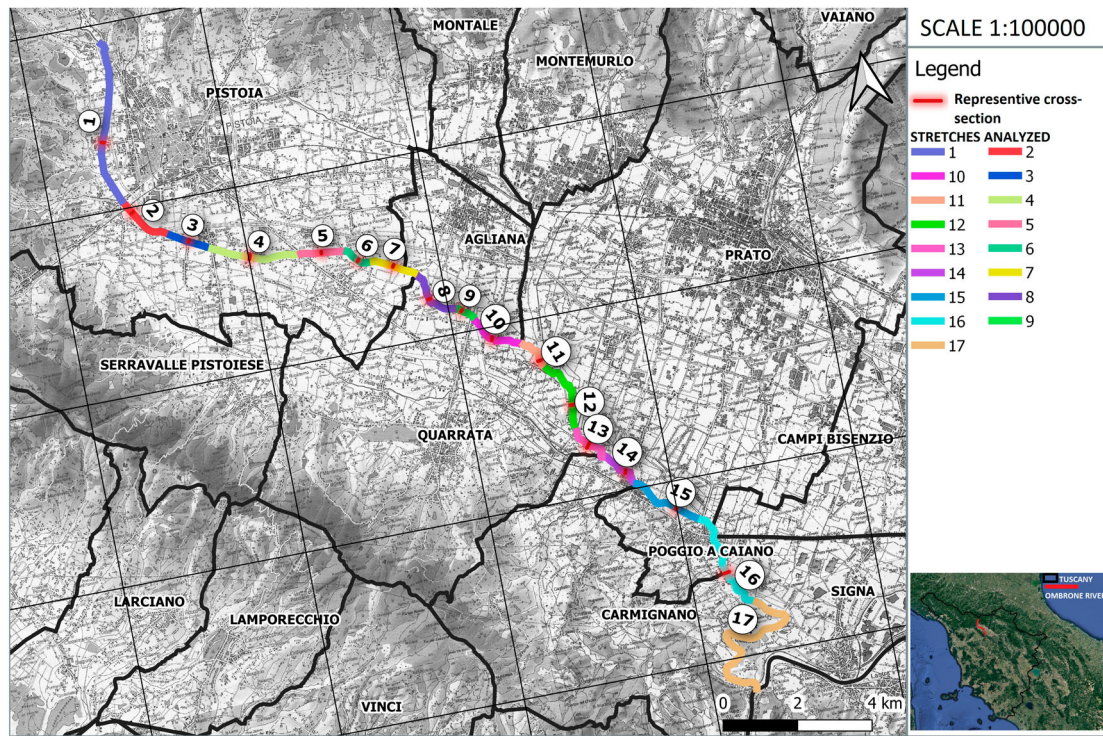


Figure 6. The study area and the location of the 17 sub-reaches.

the levee system and the morphological terrain relief. Since the flooded area is not known a priori, the spatial domain is extended as far as possible, until the local terrain elevation can contain the water volume. The analysis involves a purely 2D simulation of the flooded areas due to water flowing out of an embankment breakage, using HEC-RAS software version 5.0.7 (by US Army Corps of Engineers). The procedure consists of the following steps: (1) spatial domain modelled by using DTM; (2) land use map, to assign appropriate roughness values of the Manning coefficient; (3) assignment of boundary conditions for the unsteady flow simulation represented by the discharge hydrograph through the levee breach. As already mentioned, the discharge hydrograph outgoing from the breach has a rectangular shape with a discharge Q_{MAXBR} , which is constant over the time duration T_D .

The peak discharge Q_{MAXBR} is obtained from the criterion developed by Michelazzo (2013) and Michelazzo et al. (2018), according to which $Q_{MAXBR} = 0.6 \cdot Q_{MAX}$, where Q_{MAX} is the peak discharge of the flow in the river. The time duration T_D is defined as the persistence time T_P (Figure 4), minus the sum of breach formation time (here assumed to be 3 h) and critical time T_{CR} . Moreover, free flow is assumed to occur through the breach thus neglecting any downstream back water effect.

In this way, it is possible to evaluate the flooding areas for each river reach. Once obtained the flooded area, the risk can be defined using land use maps.

3. Case study: the Ombrone Pistoiese levee system

The Ombrone Pistoiese River is located in the north of Tuscany (Italy) (Figure 6) and joins the Arno River, after crossing the populated Pistoia-Prato plain. It has a catchment area of 489 km², a length of about 47 km and it represents one of the main water courses just downstream the city of Florence.

The Ombrone Pistoiese river is managed by the Consorzio di Bonifica Medio Valdarno n.3 (hereinafter Consorzio for brevity). The proposed methodology can provide a valid support in the development of the 'Masterplan for the adaptation of the embankment defences of the Ombrone Pistoiese between Pistoia and the outlet into the Arno River', which has to be drawn up by the Consorzio for the improvement of levee strength of the Ombrone Pistoiese River.

3.1. Historical overview

Analysis of past flood events can provide useful information on how levees have been functioning within their lifetime highlighting the major criticalities and problems in levee safety.

Historically, the Ombrone River flooded the surrounding marshy lands, causing diseases that made them uninhabitable and unproductive; this led to the construction in the 1600s of the first defence system against flooding of the river. Since then, numerous other works have been carried out by various administrations over the decades. However, the situation remains very critical at present because in many stretches the river is hanging and is characterized by intense and sudden floods. Moreover, the entire stretch extends in highly urbanized areas, where many agricultural and nursery activities are located. Coherently with what was described in the Flood Risk Management Plan (FRMP) of the District Authority (Northern Apennine District Basin Authority, 2016), developed following the indications of the Flood Directive, the historical analysis has foreseen the reconnaissance of the main criticalities that occurred in recent years. The two most catastrophic events that have occurred in the last three decades have been (Figure 5):

- The breach of the levee and the flooding of Poggio a Caiano in 1992, in which the Ombrone caused, in the



Figure 5. From left to right: the 1992 flood, the 2009 flood, the Ombrone levee breach.

right embankment in the locality of *Lombarda*, a breach of tens of metres, and consequently in a few hours the whole eastern part of Poggio a Caiano was flooded. The report counted 800 displaced families and over 300 flooded businesses, but fortunately, the flood did not cause any injuries.

- During the Christmas night of 2009, the flooding of the Ombrone caused the right embankment to break off for a length of about 20 m in the locality of *Cason dei Giacomelli* in the Municipality of Pistoia, causing flooding of the surrounding area with considerable damage to homes and production activities. The failure occurred after the first subsidence, with no overtopping.

Moreover, a careful analysis of the historical archive of the Consortium has revealed numerous criticalities along the river to the detriment of the hydraulic risk defence works. In the last five years, numerous subsidence phenomena were found to occur in the bank walls and protective shore coverings, often combined with small landslide movements of the embankments and a significant presence of animal dens.

3.2. Characteristic of the levee system

The study area includes the embankment system of the Ombrone Pistoiese River from upstream of Pistoia to the confluence in the Arno, for a dammed stretch of about 30 km. To better understand the physiography and the hydraulic dynamics of the Ombrone River, its course has been divided into 17 test sections, from the town of Pistoia to the outlet (Figure 6). The subdivision was carried out to identify stretches with an average length of 1.5 km, characterized by sections that are as homogeneous as possible within the stretch; the points at the beginning and end of the segment were identified at crossings or confluences. Exceptions are the first and last sections, which differ from

the other segments both in terms of riverbed conformation and hydraulic dynamics and involve considerably larger areas.

3.3. Seepage analysis

The first step investigates seepage through the embankments, carrying out the filtration checks of the 17 cross-sections analysed to find possible phenomena of phreatic line outcrops on the landside's surface.

The adopted scenario considers water levels calculated with a return period of 30 years with a duration of 12 h, obtained from pre-existing hydraulic modelling provided by the District Authority (Tuscany Region Authority, 2003). In this hydraulic model, the results show that the levee overflow can occur only in three simulated sub-reaches and for only one side of the river bank. The choice of the scenario is a compromise between the recurring scenarios, referring to the calamitous events of 1992 and 2009, in which floods occurred following embankment breaches for events with a return period shorter than 30 years and scenarios of significant intensity, with a return period higher than 30 years.

The permeability coefficient is affected by a high rate of variability and uncertainty, primarily due to the presence of criticalities (sandy layers, animal dens, local fragility, etc.) (Camici et al., 2014; Barbetta et al., 2017) that can increase on a local basis the value of the permeability coefficient. Considering these problems, two different values of the parameter were considered: the first, less conservative, considering a permeability coefficient equal to 1×10^{-6} m/s, deduced from previous in situ tests, carried out on the embankment structure and in the landside for hydraulic works by the Consortium; the second, more conservative, is a higher permeability coefficient, equal to 5×10^{-5} m/s.

The final output of the software VS2DTI is a graphic map, where each cell is coloured according to the degree of saturation (see Figure 7).

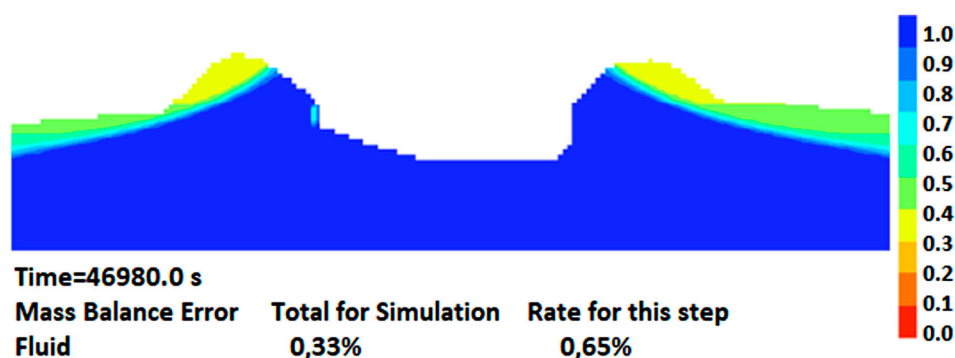


Figure 7. Seepage analysis with $k = 5 \times 10^{-5}$ m/s for 454 cross-section.

Table 3. SF of all stability tests (in bold the values that do not satisfy the limit values).

Sub-reach		Left side				Right side			
		ULS		SDLS		ULS		SDLS	
		Drained	Undrained	Drained	Undrained	Drained	Undrained	Drained	Undrained
Sec 519	Sub 1	1.63	2.45	1.98	2.5	1.26	2.63	1.45	2.72
Sec 489	Sub 2	1.1	2.2	1.54	2.84	0.82	1.5	1.08	2.61
Sec 454	Sub 3	1.24	2.34	1.82	3.28	0.83	1.79	1.38	2.7
Sec 420	Sub 4	1.06	2.21	1.7	3.04	0.71	1.99	1.21	2.82
Sec 387	Sub 5	1.11	2.34	1.95	2.9	0.79	1.71	1.42	2.71
Sec 375	Sub 6	0.88	1.72	1.52	2.19	0.67	1.53	1.31	2.34
Sec 366	Sub 7	0.84	1.68	1.49	2.39	0.49	1.38	1	1.94
Sec 350	Sub 8	0.82	1.62	1.49	2.14	0.59	1.37	1.21	2.12
Sec 341	Sub 9	0.6	1.33	1.19	1.87	0.51	1.34	1.05	2.01
Sec 320	Sub 10	0.93	1.5	1.49	1.83	0.63	1.31	1.21	1.9
Sec 298.3	Sub 11	0.95	1.74	1.52	2.09	1	1.47	1.6	1.6
Sec 287	Sub 12	0.84	1.37	1.53	1.71	0.73	1.16	1.3	1.43
Sec 262	Sub 13	1	1.34	1.62	1.56	1.01	1.44	1.72	1.73
Sec 222	Sub 14	1.3	1.53	1.85	1.75	0.76	1.42	1.43	1.91
Sec 194	Sub 15	0.75	1.24	1.47	1.53	0.73	1.08	1.37	1.29
Sec 138	Sub 16	0.92	1.25	1.6	1.44	0.75	1.17	1.41	1.45

The results of this first analysis found six of the total 32 banks affected by the outcrop of the phreatic line on the land-side's surface. Therefore, it was necessary to carry out a stability analysis to assess the value of the safety coefficient and whether it complied with the Technical Rules for Constructions parameters (hereinafter TRC for brevity) (NTC, 2018).

3.4. Slope instability analysis

In order to construct the model, a careful analysis of the geomechanical parameters was necessary. To determine them a sensitivity analysis was carried out on the geomechanical parameters of the works, such as retaining walls and protection cliffs, which are processed by the software SSAP as layer lenses and therefore require the parameters c' and Φ' (Borselli & Petri, 2020). In this study, a value of 350 kPa was assumed for the undrained cohesion relative to the bank walls. In addition, values of c' equal to 11.2 kPa and Φ' equal to 21.3° for the embankment body, and c' equal to 8 kPa and Φ' equal to 22.2° for the substrate, were assigned, using partial coefficients found in TRC 2018. The analysis was carried out both in drained and undrained conditions, for the Ultimate Limit State (ULS) and Seismic Design Limit State (SDLS) with different soil parameterization, in

the first case defined by shear resistance angle Φ' and effective cohesion c' , in the second only by undrained cohesion c_u . This choice is motivated by the fact that, as reported by Duncan et al. (2014), the adoption of one criterion rather than the other must always be justified by a thorough knowledge of geology, site conditions and mechanical properties of the soil; the available data at the moment are only preliminary and would not allow a wise choice of drainage conditions. The method used for calculating the sliding surfaces is developed for general-shaped breaking surfaces by Morgenstern-Price (1965).

The results generate a graphic map of the sliding surface with the minimum safety factor inside the embankment and by comparing the latter with the minimum coefficient required by the regulations, the study has shown that in conditions of rapid drainage, which was the most onerous condition, 80% of the 32 banks analysed do not meet the coefficient required by the regulations, as shown in Table 3.

3.5. Implementation of Collapse Propensity Index

As described in section 2.1, the study applies the proposed methodology for assessing the propensity of a soil embankment to collapse. In this case study, the return period is assumed 30 years, and T_p is obtained by the procedure described in section 2.2. The calculation of the three indexes presented in the previous paragraph leads to defining the critical condition for embankment collapse. The results from the three indexes are shown in Table 4: it should be noted that only three of the analysed banks fall into the medium hazard classes, while the remaining ones are high hazard. This is an expected result due to the relative weight of the seepage index compared to the other two, thus increasing the value of the synthetic collapse propensity index.

We found the situation of the Ombrone Pistoiese embankments to be critical along the entire stretch that extends from the reach upstream of Pistoia to the confluence in the Arno River, pointing out the need for timely intervention to restore a more stable and less risky situation.

3.6. Levee breach modelling

An assessment analysis of the potential flood-prone areas (PFPA hereinafter) due to embankment breaks, and damage

Table 4. Results of propensity index for levee collapse, for left and right bank (in bold the values of high hazard class values).

Sub-reach	Frodo index		Hanging index		Seepage index		Propensity index for Levee collapse	
	Left	Right	Left	Right	Left	Right	Left	Right
1	0.5	0.5	0	0.5	1.5	2	2	3
2	0	0	0.5	0.5	1.5	3	2	3.5
3	1	0.5	0.5	1	3	3	4.5	4.5
4	1	1	1	0.5	3	3	5	4.5
5	0.5	1	0.5	0.5	3	3	4	4.5
6	1	1	0.5	0.5	3	3	4.5	4.5
7	1	1	0.5	0.5	3	3	4.5	4.5
8	1	1	0.5	0.5	3	3	4.5	4.5
9	1	1	0.5	0.5	3	3	4.5	4.5
10	0.5	1	0.5	0.5	3	3	4	4.5
11	1	1	0	0.5	1.5	3	2.5	4.5
12	1	1	0	0.5	3	3	4	4.5
13	0	0	0.5	0	3	3	3.5	3
14	0	1	0.5	0	3	3	3.5	4
15	1	1	0	0.5	3	3	4	4.5
16	1	1	0.5	0	3	2	4.5	3

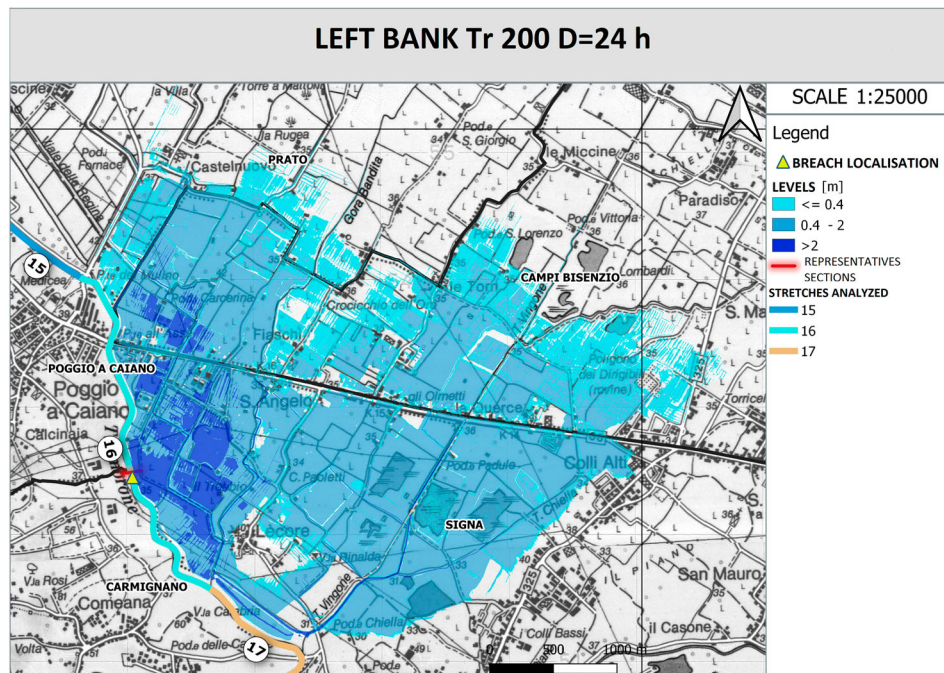


Figure 8. Example of the flooded area induced by the potential levee breach for left bank cross-section number 16.

produced on residential areas, main infrastructures, and safety-sensitive works is applied to this case study.

We used a DTM with a 1×1 m resolution that has been modified by inserting the presence of existing buildings in the analysed area. The calculation mesh was created using cells of medium size, 20×20 m throughout the territory analysed, while in correspondence of infrastructural works, such as bridges and culverts, the cells have been reduced to obtain a more accurate simulation. The other important data for the modelling was the land use map of the Region of Tuscany, used to assign the roughness values of the Manning coefficient for each area present on the territory being investigated, based on the classification drawn up by (2014). The site of the breakage was assumed to be located at the

representative section for each sub-reach (2 to 16), on the hydraulic left and right sides, for a total of 30 possible breaches along the river flow. The second step consisted in inserting the boundary conditions for the unsteady flow simulation. The upstream boundary condition is the flood hydrograph through the breach of the reference scenarios: (i) return period of 200 years and duration of the flooding equal to 9 h (catastrophic scenarios), resulting from the flooding time described before, and (ii) return period of 30 years and duration of 3 h (more frequent and less harmful scenarios). These boundary conditions are located at the representative cross-section defined in the previous steps of the procedure, paying attention to extend the modelled domain to contain all flooded areas.

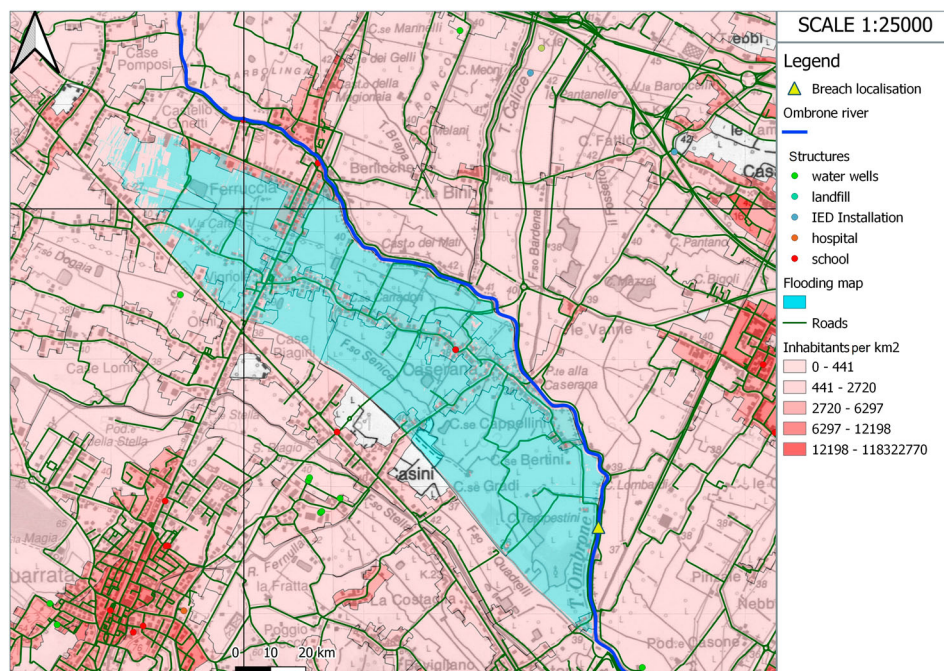


Figure 9. Structures, roads, and resident population per km^2 involved by the flood simulation (data downloaded from Region of Tuscany's website).

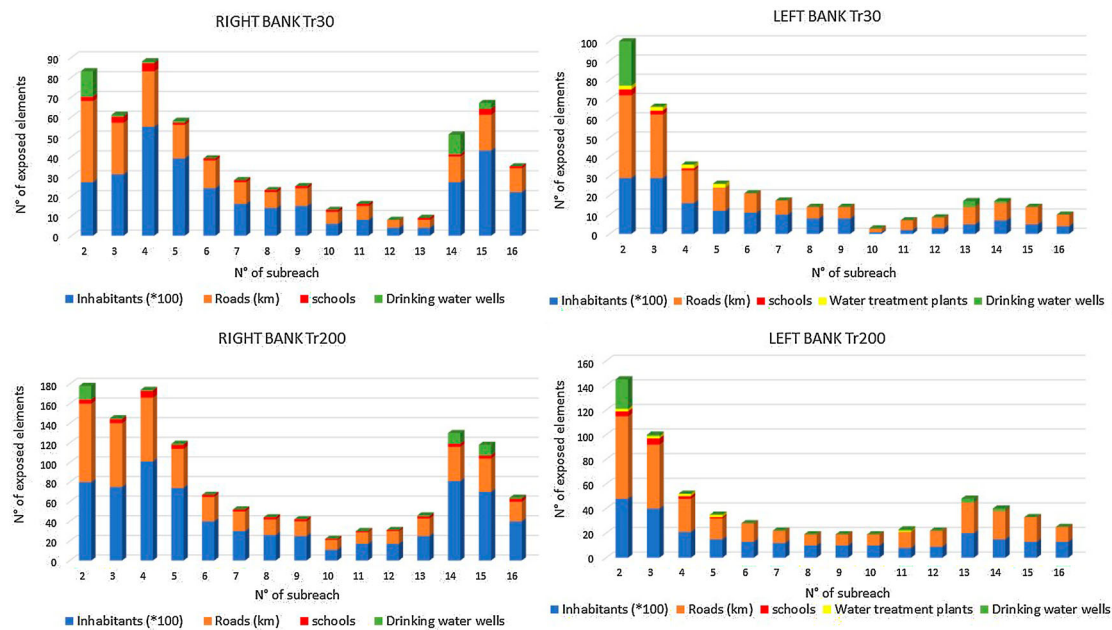


Figure 10. Summary graphs of the exposed elements number for each side bank and for each scenario: (a) right bank Tr200 years, (b) left bank Tr200 years, (c) right bank Tr30 years and (d) left bank Tr30 years.

At this point, a total of 30 hydraulic models of the potential flooding areas by embankment breach were built; one example of the results of cross-section number 16 (left bank) is shown in Figure 8. The areas affected by flooding in the upstream stretches are greater than the downstream stretches because the elevations of the areas adjacent to the levees are higher, so the flood propagation is greater. On the contrary, in the downstream valleys, the flooding area is smaller (from 2 to 5 km²), due to the stagnation phenomena in the depressed areas, as reported in Figure 8 for the last downstream section.

3.7. Identification of exposed elements within PFFA

Once the modelling was carried out, an estimation of exposures involved by the levee breaks has been made. The following data were obtained by the Region of Tuscany Geographical Office, ISTAT (national bureau of statistics), and the Northern Apennine Basin Authority: 2011 population census, road network and sensible works, such as schools, hospitals, water treatment plants, landfills, incinerators. These data were processed through QGIS software, version 3.10, to obtain an analysis of the resident population, the infrastructure and works in the flooded areas, as can be seen from Figure 9. The original shapefile data were rasterized to facilitate this type of analysis in a GIS environment.

Finally, summary graphs have been drawn up using the data obtained, showing the exposure that the breaches can involve in correspondence with the representative cross-sections (Figure 10). The following graphs show a more critical state for the upstream sub-reaches since the flooding areas are more extensive and involve more works due to the higher population density present especially in Pistoia and its surroundings. In the middle section, the trend of exposure decreases because the land surrounding the main channel is used mainly for agricultural purposes with the presence of villages. On the contrary, in the downstream stretches, the potential exposure increases due to the presence of the

small towns of Poggio a Caiano and Signa, on the hydraulic right, where both population and industrial density increase. On the other hand, the areas to the left are less exposure-prone, due to the presence of mostly farmland.

4. Discussion

The methodology proposed in the present paper is here discussed with particular emphasis on the possible limitations of the approach. Having in mind that the methodology is designed as decision support system at the basin-scale, one of the major limitations lies in the lack of analysis of the phenomena at the local scale such as river bed and bank erosion, subsidence, inhomogeneity of levee body and foundation, damages due to human and animal activity. Moreover, we remark here that only failure due to seepage process was taken into account, even if the methodology can be easily extended to include overtopping.

Regarding the time evolution of the involved processes, we assumed the breach formation time to be a constant value of 3 h based on available field data. In general, this time is difficult and almost unpredictable to define since it depends on the interaction of many factors such as flood duration, characteristics of levee body and downstream water level. The value of discharge through the breach Q_{MAXBR} is also affected by high uncertainty. Q_{MAXBR} was defined from previous laboratory test, and it was assumed constant over the time of flooding, and able to flow freely without any back water effect.

Regarding the identification of the exposed elements, the decision support system assumes that the exposed elements experience the maximum potential damages corresponding to the complete loss of the elements; of course, this is not totally true, hence this aspect could be further improved.

Finally, the exposures classes consider only the inhabitants, roads and schools affected by the flooded area: the choice of the exposed elements to be considered in the analysis, and the appropriate range of the exposure class, can be

extended to include other available data; the choice of exposed elements can be characterized for specific study area, eventually assigning in addition a weight for each exposed element.

5. Conclusion

This paper proposes a basin-scale methodology for managing flooding risk induced by levee breaches and it applies to the case study of the Ombrone Pistoiese River. The suggested methodology is a combination of classical approaches, for the calculation of seepage and the stability analysis, and more innovative approaches, applied to analyse the vulnerability of the embankment system, such as the Synthetic Collapse Propensity Index. This index is applied to 32 banks of the Ombrone Pistoiese River, showing a high-risk class for the entire area being investigated, in agreement with the embankment breach phenomena that have occurred over the last thirty years. The stability tests confirmed the current critical state of the levee system of the Ombrone Pistoiese River, with 26 out of 32 levees sites failing to meet stability safety requirements. Then, maps of potential floods following the breach of the embankments have been developed, evaluating the inundated areas in terms of inhabitants, roads and the safety-sensitive works present on them, subsequently producing summary graphs of the exposures linked to the breaches.

The proposed methodology can however be extended more generally to other case studies, and it means to represent a useful tool to be applied especially when developing a 'general masterplan' for an entire watershed for the mitigation of hydraulic risk. The masterplan, when applied to an entire river basin, is usually based on a rationale of homogeneous intervention in the medium-long term and is particularly suitable for its realization by means of 'successive functional segments', i.e. distinct and individually complete units of intervention, ordered according to a pre-defined scale of intervention priorities, to be implemented over time according to the availability of funds of the financing bodies.

Disclosure statement

No potential conflict of interest was reported by the author(s).

References

- Barbetta, S., et al (2017). Levee body seepage: A refinement of an expeditious procedure for fragility curves and vulnerability diagrams. *Hydrology Research*, 10(3), 314–325. <https://doi.org/10.2166/nh.2017.101>
- Borselli, L. (2018). Manual SSAP. <https://doi.org/10.13140/RG.2.2.12436.73604>.
- Borselli, L., & Petri, P. (2020). Muri a secco: Verifiche di stabilità con software SSAP 5.0 e criterio GHB (GSI). *Researchgate*. <https://doi.org/10.13140/RG.2.2.21048.90886/1>
- Camici, S., Barbetta, S., & Moramarco, T. (2014). Levee body vulnerability to seepage: The case study of the levee failure along the Foenna stream on 1 January 2006. *Journal of Flood Risk Management*, 10(3). <https://doi.org/10.1111/jfr3.12137>
- CE, 60/2007. (n.d.). Flood directive.
- Colleselli, F. (1994). *Problemi geotecnici relativi alle arginature ed alle sponde di fiumi e di canali*. International Centre for Mechanical Sciences.
- Collins, B., Kayen, R., Minasian, D., & Reiss, T. (2009). *Terrestrial Lidar datasets of New Orleans, Louisiana, levee failures from hurricane August 29, 2005*. U.S. Geological Survey Data Series.
- Colman, M., et al., 2016. Verso un modello di gestione del rischio arginale. Bologna: National Hydraulic conference.
- Da Deppo, L., Datei, C., & Saladin, P. (2011). *Sistemazione dei corsi d'acqua*. Edizioni Progetto Padova.
- Dazzi, S., Vacondio, R., & Mignosa, P. (2019). Integration of a levee breach erosion model in a GPU-accelerated 2D shallow water equations code. *Water Resources Research*, 55(1), 682–702. <https://doi.org/10.1029/2018WR023826>
- D'Oria, M., Maranzoni, A., & Mazzoleni, M. (2019). Probabilistic assessment of flood hazard due to levee breaches using fragility functions. *Water Resources Research*, 55(11), 8740–8764. <https://doi.org/10.1029/2019WR025369>
- Duncan, J., Wright, S., & Brandon, T. (2014). *Soil strength and slope stability* (2nd ed.). John Wiley.
- Ferrari, A., et al (2020). Enhancing the resilience to flooding induced by levee breaches in lowland areas: A methodology based on numerical modelling. *Natural Hazards and Earth System Science*, 20(1), 59–72. <https://doi.org/10.5194/nhess-20-59-2020>
- Genuchten, M. T. V. (1980). A closed-form equation for predicting the hydraulic conductivity of unsaturated soils. *Soil Science Society of America Journal*, 44(5). <https://doi.org/10.2136/sssaj1980.03615995004400050002x>
- Hall, J. W., et al (2003). A methodology for national-scale risk assessment. *Proceedings of the Institution of Civil Engineers - Water and Maritime Engineering*, 156(3), 235–247. <https://doi.org/10.1680/wame.2003.156.3.235>
- Hsieh, P. A., Wingle, W., & Healy, R. W. (2000). *VS2DI a graphical software package for simulating fluid flow and solute or energy transport in variably saturated porous media*. U.S. Geological Survey Water-Resources Investigations Report.
- Huston, D. E. A. (2011). *Pluvial (rain-related) flooding in urban areas: The invisible hazard*. Joseph Rowntree Foundation.
- Janbu, N. (1973). Slope stability computations. In R. C. Hirschfeld, & S. J. Poulos (Eds.), *Embankment dam engineering; casagrande volume* (pp. 47–86). International Journal of Rock Mechanics and Mining Sciences & Geomechanics Abstracts.
- Ko, D., & Kang, J. (2018). Experimental studies on the stability assessment of a levee using reinforced soil based on a biopolymer. *Water*, 10 (8), 1059. <https://doi.org/10.3390/w10081059>.
- Ligato, D. (2003). *Atlante delle opere di sistemazione fluviale*. APAT, Manuali e Linee guida 27/2003.
- Marchi, E. (1957). *Un criterio per la verifica alla filtrazione degli argini in terra*. Giornale del Genio Civile.
- Mazzoleni, M., Bacchi, B., Barontini, S., & Di Baldassare, G. (2014). Flooding hazard mapping in floodplain areas affected by piping breaches into the Po river. *Journal of Hydrologic Engineering*, 19 (4), 717–731. [https://doi.org/10.1061/\(ASCE\)HE.1943-5584.0000840](https://doi.org/10.1061/(ASCE)HE.1943-5584.0000840)
- Mazzoleni, M., Dottori, F., Brandimarte, L., & S, T. (2017). Effects of levee cover strength on flood mapping. *Hydrological Sciences Journal*, 62(6), 892–910. <https://doi.org/10.1080/02626667.2016.1246800>
- McBain, W. (2012). *Twenty-first century flood risk management*. Thomas Telford Limited.
- Michelazzo, G. (2013). *Breaching of river levees: analytical flow modeling and experimental hydro-morphodynamic investigations* [Thesis (PhD)]. University of Florence.
- Michelazzo, G., Oumaci, H., & Paris, E. (2018). New hypothesis for the final equilibrium stage of a river levee breach due to overflow. *Water Resources Research*, 54(7), 4277–4293. <https://doi.org/10.1029/2017WR021378>
- Michelazzo, G., Paris, E., & Solari, L. (2016). On the vulnerability of river levees induced by seepage. *Journal of Flood Risk Management*. <https://doi.org/10.1111/jfr3.12261>
- Minea, G., & Zaharia, L. (2011). Structural and non-structural measures for flood risk mitigation in the Basca river catchment. *Forum geographic*, X (1), 157–166. <https://doi.org/10.5775/fg.2067-4635.2011.034.i>
- Morgestern, N. M., & Price, V. (1965). The analysis of the stability of general slip surfaces. *Geotechnique*, 15 (1), 70–93.
- Nash, D. (1987). *A comparative review of limit equilibrium methods of stability analysis*. Slope stability Wiley, 11–75.
- Northern Appennine District Basin Authority. (2016). *The flood risk management plan*.
- NTC. (2018). Technical rules for constructions parameters. Italian Legislation.
- Orlandini, S., Moretti, G., & Albertson, J. D. (2015). Evidence of an emerging levee failure mechanism causing disastrous floods in

- Italy. *Water Resources Research*, 51(10), 7995–8011. <https://doi.org/10.1002/2015WR017426>
- Pestanana, R., Matias, M., Canelas, R., Araujo, A., Roque, D., Van Zeller, E., Trigo-Teixeira, A., Ferreira, R., Oliveira, R., & Heleno, S. (2014). *Calibration of 2D hydraulic inundation models in the flood-plain region of the Lower Tagus River*. Foundation for Science and Technology, 16.
- Sattar, M., et al (2019). Hydraulic modeling and evaluation equations for the incipient motion of sandbags for levee breach closure operations. *Water*, 11(2), 279. <https://doi.org/10.3390/w11020279>
- Serre, D., et al (2008). Levee performance assessment methods integrated in a GIS. *Journal of Infrastructures Systems*, 14(3), 201–213. [https://doi.org/10.1061/\(ASCE\)1076-0342\(2008\)14:3\(201\)](https://doi.org/10.1061/(ASCE)1076-0342(2008)14:3(201))
- Sofia, G., Masin, R., & Tarolli, P. (2017). Prospects for crowdsourced information on the geomorphic ‘engineering’ by the invasive coypu (*myocastor coypus*). *Earth Surface Processes and Landforms*, 42(2), 365–377. <https://doi.org/10.1002/esp.4081>
- Solari, L., Paris, E., & Michelazzo, G., 2014. Studi teorici e sperimentali per la valutazione della vulnerabilità arginale. Tuscany Region
- Todini, E. (2000). An operational decision support system for flood risk mapping. *Urban Water*, 1(2), 131–143. [https://doi.org/10.1016/S1462-0758\(00\)00010-8](https://doi.org/10.1016/S1462-0758(00)00010-8)
- Tourment, R., et al., 2018. European and US Levees and Flood Defences Characteristics, Risks and Governance. [Research Report] irstea.
- Tuscany Region Authority. (2003). Florence: Evaluation of the flow rates of Tuscany Region, ALTO2000 model.
- Vacondio, R., et al (2016). Simulation of the January 2014 flood on the Secchia river using a fast and high-resolution 2D parallel shallow-water numerical scheme. *Natural Hazards*, 80(1), 103–125. <https://doi.org/10.1007/s11069-015-1959-4>
- Van, M., et al, 2019. Overviewing geotechnical issues associated with levees and dams in Europe and USA Geotechnical Engineering foundation of the future. XVII ECSMGE-2019 Reykjavik 8.
- Viero, D. P., et al (2013). Mathematical modeling of flooding due to river bank failure. *Advances in Water Resources*, 59, 82–94. <https://doi.org/10.1016/j.advwatres.2013.05.011>
- Vorogushyn, S. (2010). A new methodology for flood hazard assessment considering dike breaches. *Water Resource Research*. 46 (8). <https://doi.org/10.1029/2009WR008475>.
- Vorogushyn, S., Merz, B., & Hapel, H. (2009). Development of dike fragility curves for piping and micro-instability breach mechanisms. *Natural Hazards and Earth System Sciences*, 1383–1401. <https://doi.org/10.5194/nhess-9-1383-2009>
- Zhang, L., et al (2013). Assessment of flood risks in pearl river delta due to levee breaching. *Georisk: Assessment and Management of Risk for Engineered Systems and Geohazards*, 7(2), 122–133. <https://doi.org/10.1080/17499518.2013.790733>